Numerical and asymptotic study of stresses of PTT, Giesekus and Oldroyd-B near the stick-slip singularity

José Alberto Cuminato
ICMC/USP, jacumina@icmc.usp.br

Irineu Lopes Palhares Junior
FCT/UNESP, irineu.palhares@unesp.br

October 14, 2023

FAPESP
FUNDAÇÃO DE AMPARO À PESQUISA DO ESTADO DE SÃO PAULO

Summary

Motivation

- The extrusion process of viscoelastic fluids is a crucial phenomenon encountered in numerous industrial applications [1].
- A comprehensive grasp of the stick-slip flow problem provides valuable insights into the mechanics of extrudate swelling.
- The stick-slip problem is often regarded as a benchmark problem due to its simple geometry but numerical complexity, as highlighted in [2].
- The presence of a stress singularity serves as a test for rheological models, and it remains unclear whether all constitutive equations behave appropriately under extremely high stress conditions.
- An understanding of asymptotic behavior can enhance the discretization and accuracy of numerical schemes, as exemplified in [3] and [6].
- The asymptotic analysis elucidated the behavior near singularities, a phenomenon corroborated by the numerical findings.

The stick-slip problem

- In this flow scenario, there is an abrupt transition in flow boundary conditions, shifting from no-slip to zero shear. This alteration in boundary conditions leads to the emergence of a singular point at the die-exit, as depicted in Figure 1 (a). This particular fluid flow phenomenon is commonly referred to as the stick-slip problem [18].

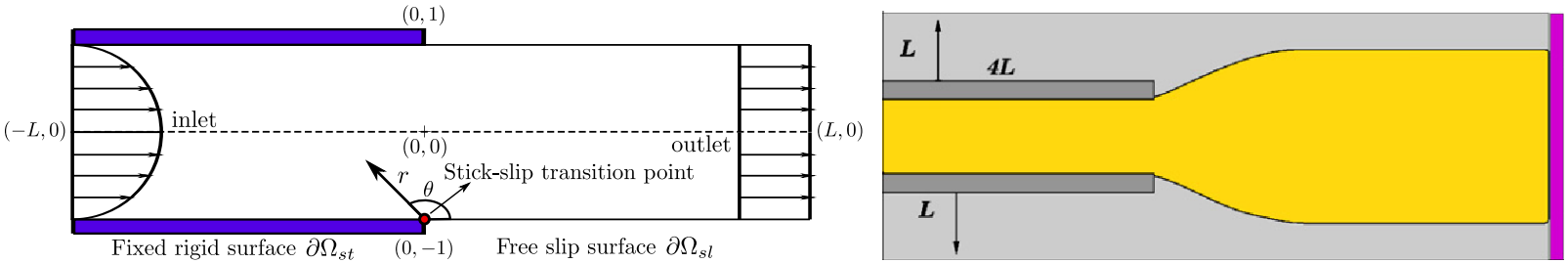

Stick-slip Die-swell

Figure 1: (a) The stick-slip geometry description and (b) the die-swell flow [16].

Governing equations

The governing equations to this flow are described bellow:

- Momentum

$$\frac{\partial \mathbf{v}}{\partial t} + (\mathbf{v}.\nabla)\,\mathbf{v} = -\frac{1}{Re}\nabla p + \frac{\beta}{Re}\nabla^2 + \frac{1}{Re}\nabla.\mathbf{T}^p \tag{1}$$

- Continuity

$$\nabla.\mathbf{v} = 0 \tag{2}$$

- Constitutive equation

$$\frac{\partial \mathbf{T}^p}{\partial t} + (\mathbf{v}.\nabla)\,\mathbf{T}^p - \left(\nabla\mathbf{v}\mathbf{T}^p + \mathbf{T}^p\nabla\mathbf{v}^T\right) + \frac{1}{Wi}\mathbf{T}^p + \frac{\kappa}{1-\beta}g\left(\mathbf{T}^p\right) = 2\frac{1-\beta}{Wi}\mathbf{D}, \tag{3}$$

where

$$g(\mathbf{T}) = \begin{cases} 0, & \text{Oldroyd-B} \\ tr\left(\mathbf{T}^p\right)\mathbf{T}^p, & \text{PTT} \\ \left(\mathbf{T}^p\right)^2, & \text{Giesekus} \end{cases} \tag{4}$$

Natural Stress Formulation

The polymer stress tensor $\mathbf{T}^p$ can be expanded as

$$\mathbf{T}^p = \frac{1-\beta}{Wi}\left(\lambda \mathbf{v}\mathbf{v}^T + \mu\left(\mathbf{v}\mathbf{w}^T + \mathbf{w}\mathbf{v}^T\right) + \nu \mathbf{w}\mathbf{w}^T - \mathbf{I}\right), \tag{5}$$

where

$$\mathbf{v} = (u, v), \quad \mathbf{w} = \left(-\frac{v}{\|\mathbf{v}\|^2}, \frac{u}{\|\mathbf{v}\|^2}\right). \tag{6}$$

This expansion was first presented by Renardy [11] and it was used to avoid down-stream instabilities near the re-entrant corner. The idea behind the expansion is to align the stresses with the streamlines. We applied it in order to try improving the accuracy of our numerical method near the singularity for the stick-slip problem.

Constitutive equation in natural basis

The natural stress equations are given by

$$
\begin{aligned}
\frac{D\lambda}{Dt} &= -\frac{2}{\|\mathbf{v}\|^2}\left[\frac{\partial u}{\partial t}\left(\lambda u + \mu\frac{v}{\|\mathbf{v}\|^2}\right) + \frac{\partial v}{\partial t}\left(\lambda v - \mu\frac{u}{\|\mathbf{v}\|^2}\right)\right] - 2\mu\nabla.\mathbf{w} + \\
&\frac{1}{Wi}\left(\frac{1}{\|\mathbf{v}\|^2} - \lambda\right) - \frac{\kappa}{Wi}g_\lambda, \\
\frac{D\mu}{Dt} &= \frac{\partial u}{\partial t}\left(\lambda v - \nu\frac{v}{\|\mathbf{v}\|^4}\right) + \frac{\partial v}{\partial t}\left(-\lambda u + \nu\frac{u}{\|\mathbf{v}\|^4}\right) - \nu\nabla.\mathbf{w} - \frac{\mu}{Wi} - \frac{\kappa}{Wi}g_\mu, \\
\frac{D\nu}{Dt} &= 2\left[\frac{\partial u}{\partial t}\left(\mu v + \nu\frac{u}{\|\mathbf{v}\|^2}\right) + \frac{\partial v}{\partial t}\left(-\mu u + \nu\frac{v}{\|\mathbf{v}\|^2}\right)\right] + \frac{1}{Wi}\left(\|\mathbf{v}\|^2 - \nu\right) - \frac{\kappa}{Wi}g_\nu,
\end{aligned}
\tag{7}
$$

where

$$
g_\lambda = \begin{cases} 0, & \text{Oldroyd-B} \\ \left(\lambda\|\mathbf{v}\|^2 - 2 + \frac{\nu}{\|\mathbf{v}\|^2}\right)\left(\lambda - \frac{1}{\|\mathbf{v}\|^2}\right), & \text{PTT} \\ \left(\lambda - \frac{1}{\|\mathbf{v}\|^2}\right)^2\|\mathbf{v}\|^2 + \frac{\mu^2}{\|\mathbf{v}\|}^2, & \text{Giesekus} \end{cases}
\qquad
g_\mu = \begin{cases} 0, & \text{Oldroyd-B} \\ \left(\lambda\|\mathbf{v}\|^2 - 2 + \frac{\nu}{\|\mathbf{v}\|^2}\right)\mu, & \text{PTT/Giesekus} \end{cases}
$$

$$
g_\nu = \begin{cases} 0, & \text{Oldroyd-B} \\ \left(\lambda\|\mathbf{v}\|^2 - 2 + \frac{\nu}{\|\mathbf{v}\|^2}\right)\left(\nu - \|\mathbf{v}\|^2\right), & \text{PTT} \\ \left(\nu - \|\mathbf{v}\|^2\right)^2\frac{1}{\|\mathbf{v}\|^2} + \mu^2\|\mathbf{v}\|^2, & \text{Giesekus.} \end{cases}
\tag{8}
$$

Asymptotic results

The stream function for the Stokes flow is given by

$$\psi = 2C_0 r^{\frac{3}{2}} \sin\left(\frac{\theta}{2}\right) \sin(\theta), \quad \text{as } r \to 0. \tag{9}$$

The asymptotic results for the Oldroyd-B [7], PTT [4] and Giesekus [5] (using a Newtonian velocity field) are

$$\mathbf{T}^p \sim \begin{cases} r^{-\frac{4}{5}}, & \text{Oldroyd-B} \\ r^{-\frac{4}{11}}, & \text{PTT} \\ r^{-\frac{5}{16}}, & \text{Giesekus} \end{cases} \tag{10}$$

and

$$\lambda = \begin{cases} O\left(r^{-\frac{9}{5}}\right), & \text{Oldroyd-B} \\ O\left(r^{-\frac{15}{11}}\right), & \text{PTT} \\ O\left(r^{-\frac{21}{16}}\right), & \text{Giesekus} \end{cases}, \quad \mu = \begin{cases} O\left(r^{-\frac{3}{10}}\right), & \text{Oldroyd-B} \\ O\left(r^{-\frac{3}{22}}\right), & \text{PTT} \\ O\left(r^{0}\right), & \text{Giesekus} \end{cases}, \quad \nu = \begin{cases} O\left(r^{\frac{6}{5}}\right), & \text{Oldroyd-B} \\ O\left(r^{\frac{12}{11}}\right), & \text{PTT} \\ O\left(r^{\frac{21}{16}}\right), & \text{Giesekus} \end{cases} \tag{11}$$

Integration along streamlines: simplifications

The streamlines are the level curves of the function $\psi = C_0 r^{\frac{3}{2}} f(\theta)$ and parameterise each streamline by θ, we have

$$r = \left(\frac{\psi}{C_0 f(\theta)} \right)^{\frac{2}{3}}. \tag{12}$$

Since $\frac{dr}{r d\theta} = \frac{v_r}{v_\theta}$, then

$$\mathbf{v}.\nabla = \frac{v_\theta}{r} \frac{d}{d\theta}, \tag{13}$$

where $\frac{d}{d\theta}$ is the total derivative with respect to θ along the streamline.

Constitutive equations as a system of ordinary differential equation

Substituting Eq. (13) into the constitutive equations (3) yields

$$
\begin{aligned}
&\frac{dT^p_{rr}}{d\theta} - 2\frac{\partial v_r}{\partial r}T^p_{rr} - \frac{2}{r}\frac{\partial v_r}{\partial \theta}T^p_{r\theta} + \kappa g_{rr} + \frac{T^p_{rr}}{Wi} = \frac{2}{Wi}\frac{\partial v_r}{\partial r},\\
&\frac{dT^p_{r\theta}}{d\theta} + \frac{v_\theta}{r}T^p_{rr} - \frac{1}{r}\frac{\partial v_r}{\partial \theta}T^p_{\theta\theta} - \frac{\partial v_\theta}{\partial r}T^p_{rr} + \kappa g_{r\theta} + \frac{T^p_{r\theta}}{Wi} = \frac{1}{Wi}\left(\frac{1}{r}\frac{\partial v_r}{\partial r} - \frac{v_\theta}{r} + \frac{\partial v_\theta}{\partial r}\right),\\
&\frac{dT^p_{\theta\theta}}{d\theta} + 2\frac{v_\theta}{r}T^p_{r\theta} - 2\frac{\partial v_\theta}{\partial r}T^p_{r\theta} - \frac{2}{r}\frac{\partial v_\theta}{\partial \theta} - 2\frac{v_r}{r}T^p_{\theta\theta} + \kappa g_{\theta\theta} + \frac{T^p_{\theta\theta}}{Wi} = \frac{2}{Wi}\left(\frac{1}{r}\frac{\partial v_\theta}{\partial \theta} + \frac{v_r}{r}\right).
\end{aligned}
\tag{14}
$$

The system of ode for the NSF is provided as follows:

$$
\begin{aligned}
&\frac{v_\theta}{r}\frac{d\lambda}{d\theta} + 2\mu\nabla.\mathbf{w} + \frac{\kappa}{Wi}g_\lambda = \frac{1}{Wi}\left(\frac{1}{\|\mathbf{v}\|^2} - \lambda\right),\\
&\frac{v_\theta}{r}\frac{d\mu}{d\theta} + \nu\nabla.\mathbf{w} + \frac{\kappa}{Wi}g_\mu = \frac{1}{Wi}\left(\frac{1}{\|\mathbf{v}\|^2} - \lambda\right),\\
&\frac{v_\theta}{r}\frac{d\nu}{d\theta} + \frac{\kappa}{Wi}g_\nu = \frac{1}{Wi}\left(\frac{1}{\|\mathbf{v}\|^2} - \lambda\right).
\end{aligned}
\tag{15}
$$

Integration along streamlines

For a numerical solution, we fix the streamline, i.e. the value of ψ and solve the resulting system of ode's (equation (14) or (15)). The interval of integration for θ is take as $\left[10^{-6}, \pi - 10^{-10}\right]$ and use Matlab's ode15s solver with $AbsTol = RelTol = 10^{-6}$.

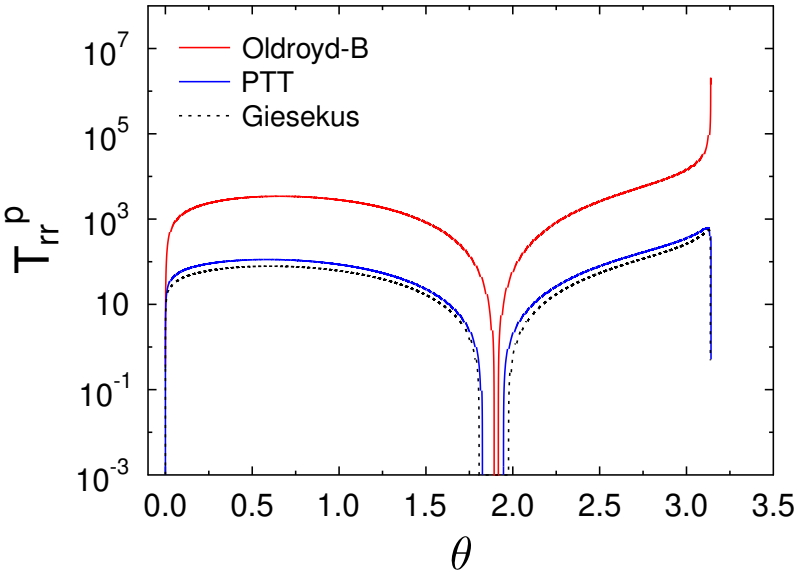

Figure 2: T^p_{rr}-component of $\mathbf{T}^p$ along the streamline $\psi = -10^{-6}$.

Verification of the asymptotic results for the CSF

Verification of the asymptotic results of the stress components of $\mathbf{T}^p$:

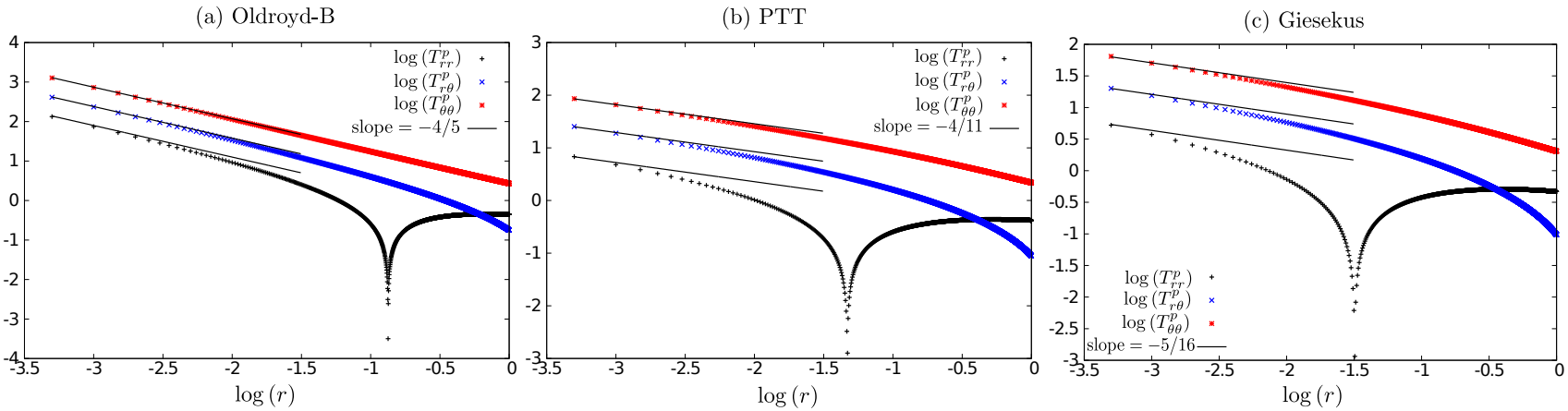

Figure 3: Verification of the singularity behaviour for the (a) Oldroyd-B, (b) PTT and (c) Giesekus model along the line $\theta = \frac{\pi}{2}$ using the CSF.

Verification of the asymptotic results for the NSF

Verification of the asymptotic results for natural stress variables:

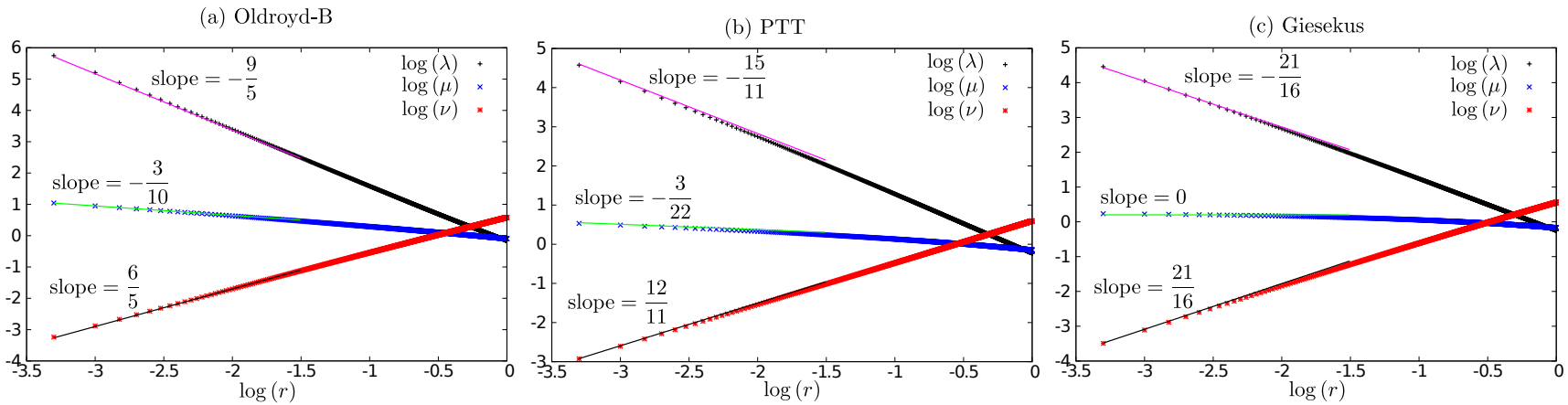

Figure 4: Verification of the singularity behaviour for the (a) Oldroyd-B, (b) PTT and (c) Giesekus model along the line $\theta = \frac{\pi}{2}$ using the NSF.

Integration of the constitutive equations using the complete set of equations

The numerical algorithm is outlined as follows:

- Momentum and continuity equations (1) and (2) are uncoupled via the incremental projection method [16]

$$\mathbf{v}^{n+1} = \tilde{\mathbf{v}}^{n+1} - \nabla\phi^{n+1} \tag{16}$$

  So that, the momentum equation is solved for a tentative velocity field $\tilde{\mathbf{v}}^{n+1}$.

- The parameter ϕ is calculated by solving a Poisson-like equation

$$\nabla^2\phi^{n+1} = \nabla.\tilde{\mathbf{v}}^{n+1} \tag{17}$$

- The pressure field is taken as

$$p^{n+1} = p^n + \frac{Re}{\Delta t}\phi^{n+1} \tag{18}$$

- Finally, the constitutive equation is calculated using the explicity Euler method.

Numerical study of temporal convergence for the CSF

The evolution of the residuals of u and stress components over time is as follows:

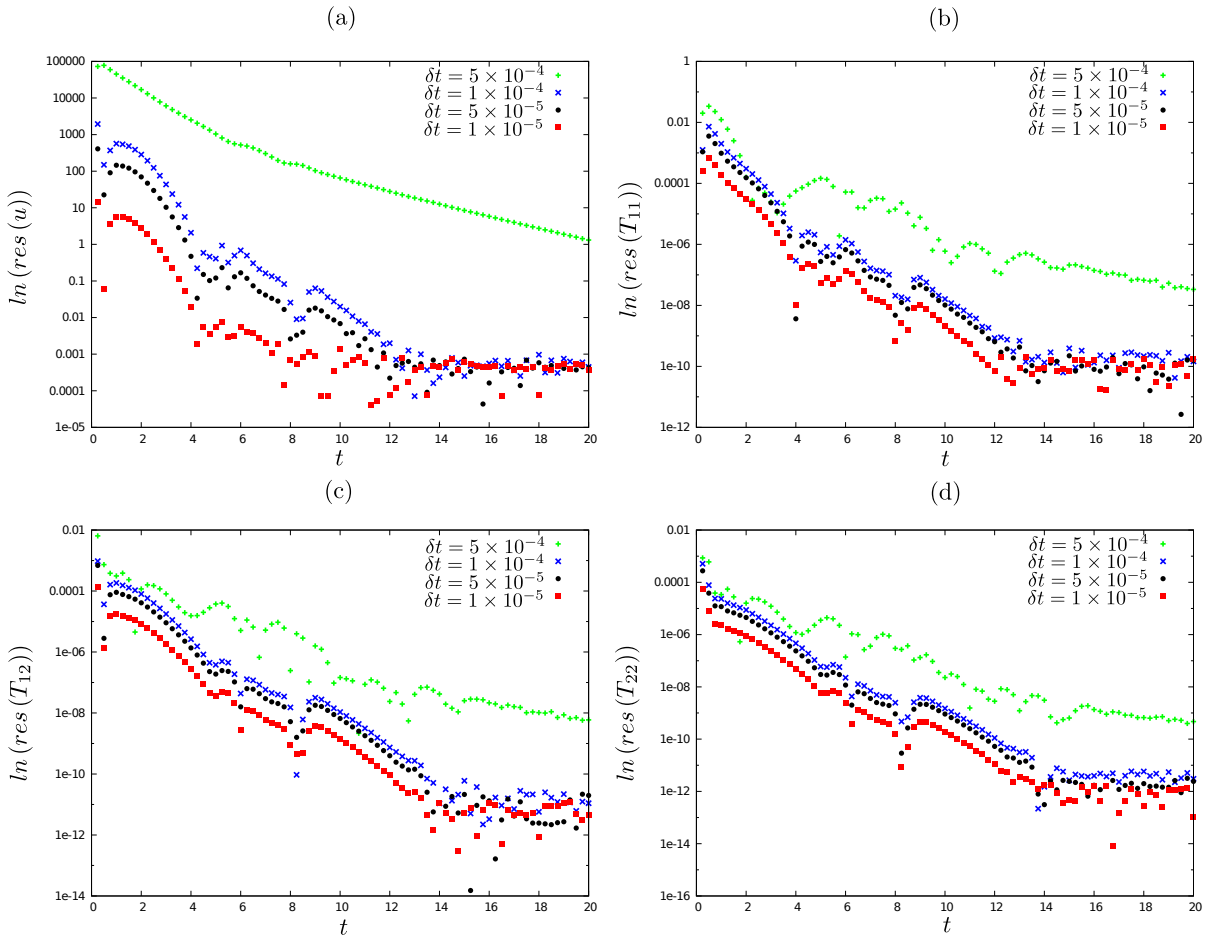

Figure 5: Time variation of the CSF local residuals of (a) u, (b) T^p_{11}, (c) T^p_{12} and (d) T^p_{22} near to the singularity of the PTT model using $\beta = \frac{1}{2}$.

Numerical study of temporal convergence for the NSF

The evolution of the residuals of u and natural stress variables over time is as follows:

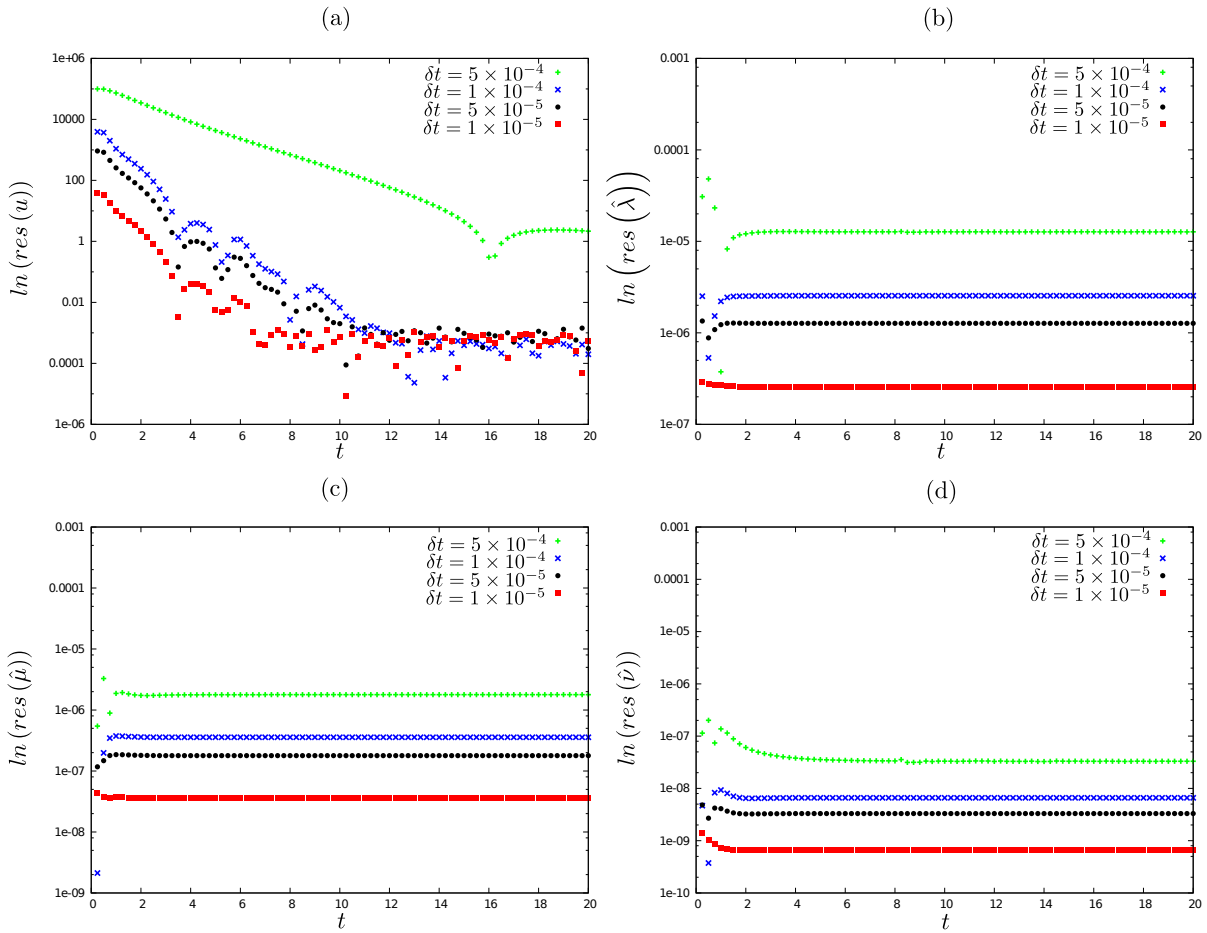

Figure 6: Time variation of the NSF local residuals of (a) u, (b) λ, (c) μ and (d) ν near to the singularity of the PTT model using $\beta = \frac{1}{2}$.

Numerical comparison with the asymptotic results

Verification of the asymptotic behavior of u, v, and p:

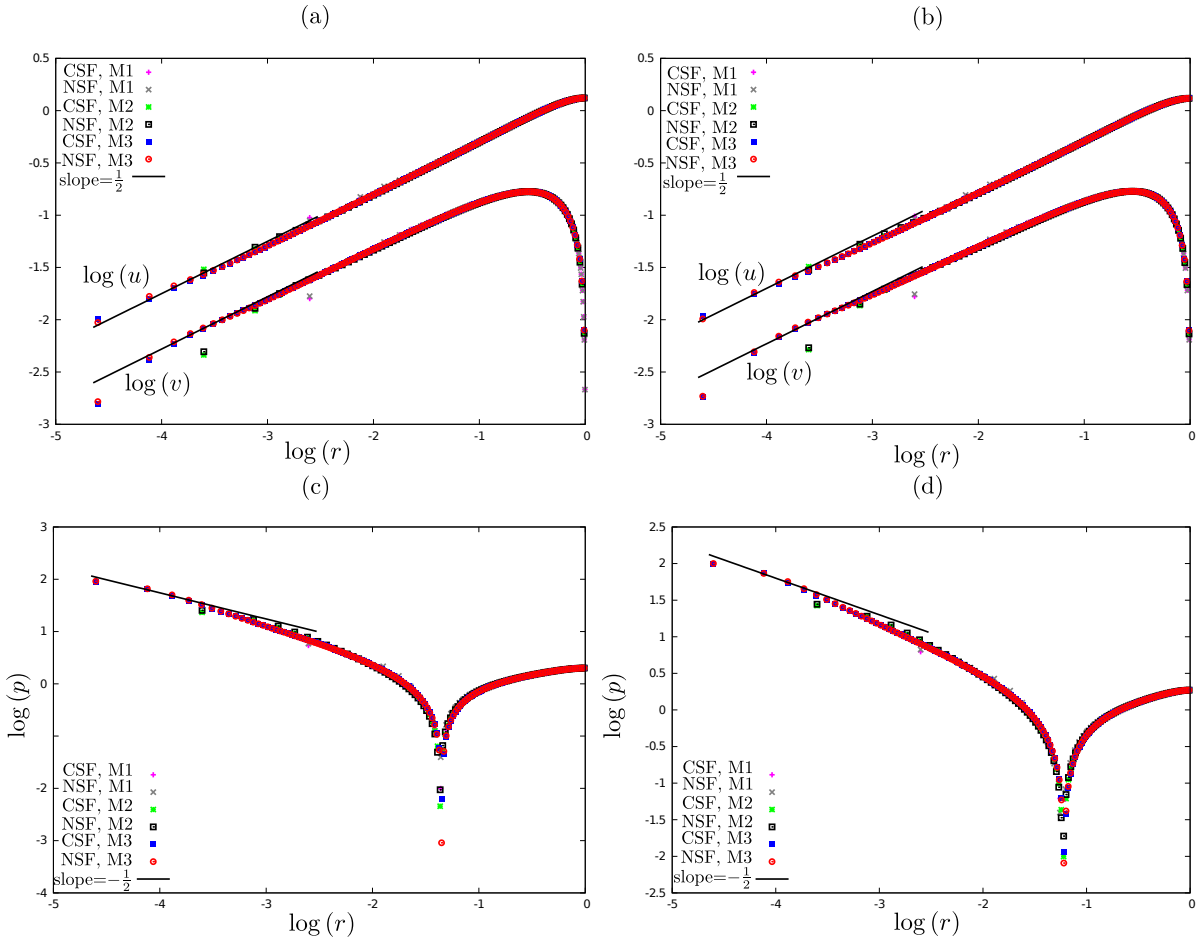

Figure 7: Asymptotic variation near the stick-slip transition point of (a) u, v (PTT), (b) u, v (Giesekus), (c) p (PTT) and (d) p (Giesekus) along the line $\theta = \frac{\pi}{2}$ with $\beta = \frac{1}{2}$.

Numerical comparison with the asymptotic results

Verification of the asymptotic behavior of the stress components and the natural stress variables:

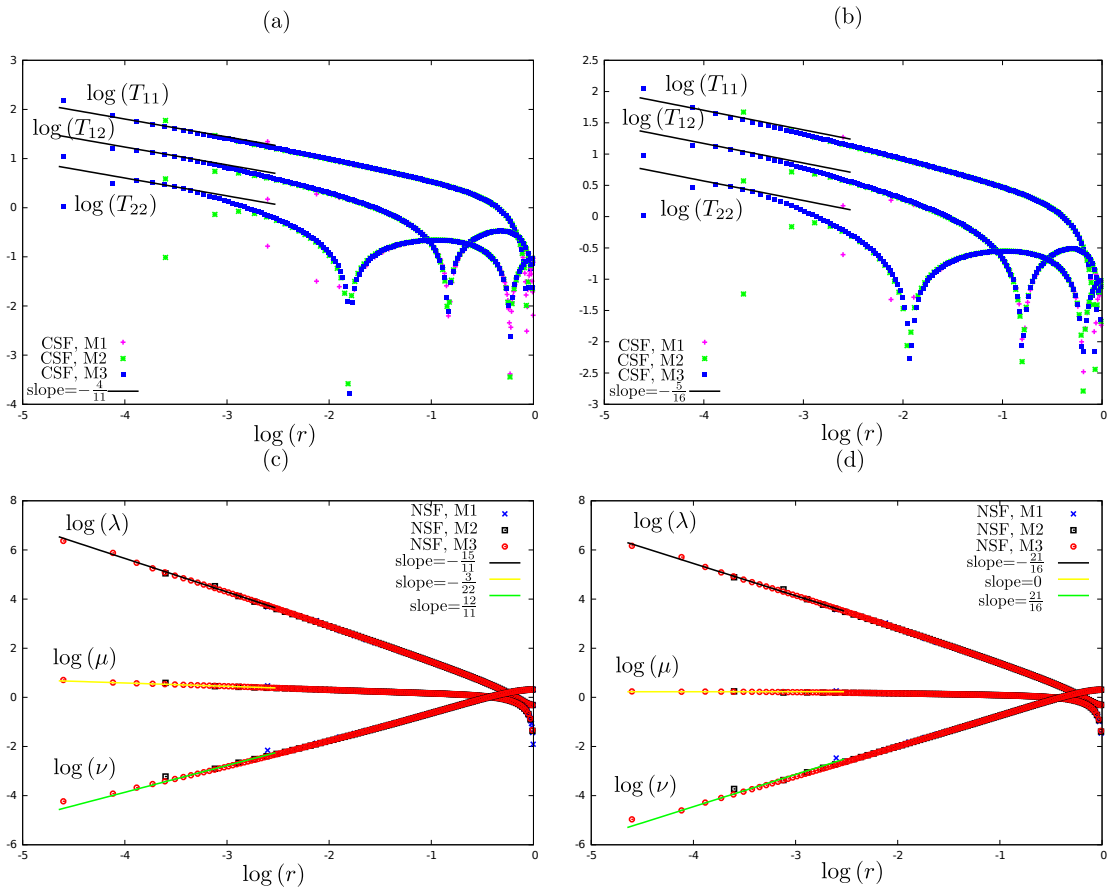

Figure 8: Asymptotic variation near the stick-slip transition point of (a) T_{11}^p, T_{12}^p, T_{22}^p (PTT), (b) T_{11}^p, T_{12}^p, T_{22}^p (Giesekus), (c) λ, μ, ν (PTT) and (d) λ, μ, ν (Giesekus) along the line $\theta = \frac{\pi}{2}$ with $\beta = \frac{1}{2}$.

Conclusions

- The asymptotic results for the stress singularity in the context of the Oldroyd-B, PTT, and Giesekus models have been substantiated through numerical validation within a prescribed Newtonian velocity field.
- Numerical analysis of the Oldroyd-B model suggests that it lacks inherent mechanisms within its equations to hinder the growth of stress at the slip surface.
- The computational scheme is capable of solving the transient problem and has been applied to two distinct formulations of polymer constitutive equations: CSF and NSF.
- The primary finding from the numerical tests underscores the remarkable enhancement in both temporal convergence rates for the extra-stress residuals and spatial accuracy in capturing the stress singularity behavior, particularly achieved by the NSF formulation over the CSF formulation.

[1] R. J. Tanner, Engineering Rheology. OUP, (1985).

[2] O. Hassager, Working group on numerical techniques, in Proceedings of the Vth Workshop on Numerical Methods in Non-Newtonian Flow, J. Non-Newtonian Fluid Mech., vol. 29, pp. 2-5, (1988).

[3] M. Elliotis, G. Georgiou, and C. Xenophontos, Solution of the planar Newtonian stick-slip problem with the singular function boundary integral method, International jornal for numerical methods in fluids, vol. 48, n9, pp. 1001-1021, 2005.

[4] J. Evans, Stick-slip and slip-stick singularities of the Phan-Thien Tanner fluid, Journal Non-Newtonian Fluids Mechanics, vol. 199, pp. 12-19, 2013.

[5] J. Evans, Stick-slip singularity of the Giesekus fluid, Journal Non-Newtonian Fluid Mechanics, vol. 222, pp. 24-33, 2015.

[6] J. D. Evans and C. M. Oishi, Transient computations using the natural stress formulation for solving sharp corner flows, Journal Non-Newtonian Fluids Mechanics, vol. 249, pp. 48-52, 2017.

[7] J. D. Evans, I. L. Palhares Junior, C. M. Oishi. Stresses of PTT, Giesekus, and Oldroyd-B fluids in a Newtonian velocity field near the stick-slip singularity. Physics of Fluids, 29(12) (2017).

[8] J. D. Evans, J. A. Cuminato, I. L. Palhares Junior, C. M. Oishi. Numerical study of the stress singularity in stick-slip flow of the Phan-Thien Tanner and Giesekus fluids. Physics of Fluids, 31(9) (2019).

[9] J. D. Evans, H. L. França, C. M. Oishi, Application of the natural stress formulation for solving unsteady viscoelastic contraction flows, Journal of Computational Physics. 388 (2019) 462-489.

[10] J. D. Evans, H. L. França, I. L. Palhares Junior, C. M. Oishi. Testing viscoelastic numerical schemes using the Oldroyd-B fluid in Newtonian kinematics. Applied Mathematics and Computation, (2020) 387, 125106.

[11] M. Renardy, How to integrate the upper convected Maxwell (UCM) stresses near a singularity (and maybe elsewhere, too). J. Non-Newtonian Fluid Mech. 52(1) (1994) 91-95.

[12] W.R. Dean, P.E. Montagnon, On the steady motion of viscous liquid in a corner, Proc. Cambridge Philos. Soc. 45 (1949) 389-394.

[13] H.K. Moffatt, Viscous and resistive eddies near a sharp corner, J. Non-Newtonian Fluid Mech. 18 (1964) 1-18.

[14] J. D. Evans. Re-entrant corner behaviour of the PTT fluid with a solvent viscosity. J. Non-Newtonian Fluid Mech., 165 (2010) 527-537.

[15] J. D. Evans. Re-entrant corner behaviour of the Giesekus fluid with a solvent viscosity. J. Non-Newtonian Fluid Mech., 165 (2010) 538-543.

[16] C. M. Oishi, F. P. Martins, M. F. Tome, J. A. Cuminato, and S. Mckee, Numerical solution of the extended pom-pom model for viscoelastic free surface flows, Journal of Non-Newtonian Fluid Mechanics, vol. 166, n. 3, pp. 165-179, 2011.

[17] M. Renardy. The stresses of an upper convected Maxwell fluid in a Newtonian velocity field near a re-entrant corner. J. Non-Newtonian Fluid Mech., 50 (1993) 127–134.

[18] S. Richardson. A 'stick-slip'problem related to the motion of a free jet at low Reynolds numbers. In Mathematical Proceedings of the Cambridge Philosophical Society. 67 (1970) 477-489.

[19] Michael, D. H. "The separation of a viscous liquid at a straight edge." Mathematika 5.1 (1958): 82-84.

[20] Oishi, Cassio M., et al. "Numerical solution of the eXtended Pom-Pom model for viscoelastic free surface flows." Journal of Non-Newtonian Fluid Mechanics 166.3-4 (2011): 165-179.